Published OnlineFirst December 27, 2012; DOI: 10.1158/1535-7163.MCT-12-0780

Selective Photodetection and Photodynamic Therapy for Prostate Cancer through Targeting of Proteolytic Activity

Maria-Fernanda Zuluaga[1], Nawal Sekkat[1], Doris Gabriel[1], Hubert van den Bergh[2], and Norbert Lange[1]

Abstract

Frequent side effects of radical treatment modalities and the availability of novel diagnostics have raised the interest in focal therapies for localized prostate cancer. To improve the selectivity and therapeutic efficacy of such therapies, we developed a minimally invasive procedure based on a novel polymeric photosensitizer prodrug sensitive to urokinase-type plasminogen activator (uPA). The compound is inactive in its prodrug form and accumulates passively at the tumor site by the enhanced permeability and retention effect. There, the prodrug is selectively converted to its photoactive form by uPA, which is overexpressed by prostate cancer cells. Irradiation of the activated photosensitizer exerts a tumor-selective phototoxic effect. The prodrug alone (8 μmol/L) showed no toxic effect on PC-3 cells, but upon irradiation the cell viability was reduced by 90%. *In vivo*, after systemic administration of the prodrug, PC-3 xenografts became selectively fluorescent. This is indicative of the prodrug accumulation in the tumor and selective local enzymatic activation. Qualitative analysis of the activated compound confirmed that the enzymatic cleavage occurred selectively in the tumor, with only trace amounts in the neighboring skin or muscle. Subsequent photodynamic therapy studies showed complete tumor eradication of animals treated with light (150 J/cm^2 at 665 nm) 16 hours after the injection of the prodrug (7.5 mg/kg). These promising results evidence the excellent selectivity of our prodrug with the potential to be used for both imaging and therapy for localized prostate cancer. *Mol Cancer Ther; 12(3); 306–13. ©2012 AACR.*

Introduction

Prostate cancer is the most prevalent cancer in the male population (1). The gold standard for the treatment of localized disease is radical prostatectomy or radiotherapy. A minority of low-risk patients can be kept under active surveillance, but this often only delays the final treatment (2). The excellent results obtained with the radical treatment come at the cost of frequent side effects (mainly sexual or urinary dysfunction) and their long-lasting impact on the quality of life. Mapping biopsies and imaging with endorectal coil MRI have laid the foundation for local therapies, which might cause fewer side effects.

Current options for localized therapy include brachytherapy, cryotherapy, high intensity focused ultrasound, laser ablation, and photodynamic therapy (PDT; ref. 3).

The latter requires 3 main elements: a photosensitizer, light, and oxygen. After administration, the photosensitizer accumulates to some extent in the target tissue and subsequently can be selectively activated by light to produce reactive oxygen species. With recent progress in light delivery and dosimetry, the use of PDT is no longer restricted to the skin. Fairly superficial lesions in hollow organs can be treated (4, 5) and prostate cancer is also open to PDT if one inserts optical devices into the lesions.

HpD, a hematoporphyrin derivative, which is a complex mixture of porphyrins was among the first photosensitizers assessed clinically. This was followed by the use of a somewhat purified mixture called Photofrin that was used to treat prostate cancer (6). Subsequently, small prospective clinical trials using Foscan (7) and 5-aminolevulinic acid (8), have been reported. Despite promising PDT responses, one observed prolonged skin sensitization in the case of Foscan and occasional extraprostatic tissue injury. This encouraged further research efforts, which aimed mainly at improving PDT selectivity and reducing side effects. In this context, LuTex and Tookad specifically targeting the vasculature

Authors' Affiliations: [1]Department of Pharmaceutics and Biopharmaceutics, School of Pharmaceutical Sciences, University of Geneva, University of Lausanne, Geneva; and [2]Photomedicine Group, Institute of Bioengineering, Swiss Federal Institute of Technology (EPFL), Lausanne, Switzerland

Note: Supplementary data for this article are available at Molecular Cancer Therapeutics Online (http://mct.aacrjournals.org/).

Current addresses for D. Gabriel: Department of Chemical Engineering, Massachusetts Institute of Technology, Cambridge, MA 02139; and Department of Anesthesiology, Division of Critical Care, Children's Hospital Boston, Harvard Medical School, Boston, MA 02115.

Corresponding Author: Norbert Lange, Department of Pharmaceutics and Biopharmaceutics, School of Pharmaceutical Sciences, University of Geneva, University of Lausanne, 30 Quai Ernest-Ansermet, 1211 Geneva 4, Switzerland. Phone: 41-22-37-933-35; Fax: 41-22-37-965-67; E-mail: Norbert.Lange@unige.ch

doi: 10.1158/1535-7163.MCT-12-0780

Published OnlineFirst December 27, 2012; DOI: 10.1158/1535-7163.MCT-12-0780

combined with local light delivery to the prostate were evaluated (9). Trials for the treatment of primary and recurrent prostate cancer using these agents showed good tolerability. However, some patients did not respond to the treatment or presented urinary and rectal damage (10–13). Even with the improved formulation of Tookad, insufficient therapeutic responses and collateral damage have been reported recently (Emberton, IPA Congress, Innsbruck, 2011).

Therefore, improvements in the tumor selective delivery of photosensitizer are needed to avoid collateral damage of the urethra, rectum, and urinary sphincter (14). With this goal in mind, we have developed polymeric protease-sensitive photosensitizer prodrugs (PPP) following a triple targeting strategy: (i) selective delivery of the PPP into tumor tissue is promoted by the polymeric carrier through the enhanced permeability and retention effect (15). In its prodrug form, photoactivity is impeded through efficient intramolecular quenching between closely positioned photosensitizer molecules on the polymeric carrier. (ii) Proteolytic activation occurs via cleavage of the peptide linkers by urokinase-type plasminogen activator (uPA), which is overexpressed by prostate cancer cells (16). Release from the polymeric backbone thus reestablishes the photosensitizer's photoactivity selectively in the target tissue. (iii) Local irradiation further increases selectivity and induces toxic radicals.

In a previous study, we have reported on a prodrug candidate (uPA-PPP-4) capable of accumulating in prostate cancer tumors and being activated by upregulated uPA (17). The present report investigates the therapeutic potential of this prodrug by evaluating its phototoxic effect *in vitro* in PC-3 and luciferase-transfected PC-3M-luc-C6 cancer cells as well as *in vivo* in a prostate cancer xenograft model.

Materials and Methods

Compounds

uPA-PPP-4 (Fig. 1) consisted of multiple copies of the photosensitizer pheophorbide a (Pb*a*) attached to a poly-L-lysine backbone via a GSGRSAG peptide sequence. It was synthesized and characterized as described previously (17, 18) as well as in more detail in the Supplementary Materials and Methods. The purity of the prodrug was confirmed by reversed phase high-performance liquid chromatography, with monitoring at 280, 330, and 450 nm. A prodrug mass of approximately 108 kDa was confirmed by SEC-MALLS-RI-UV using a column Waters Ultrahydrogel linear (column temperature: 35°C ± 0.2°C; mobile phase: 0.15 mol/L acetic acid, 0.1 mol/L sodium acetate, 0.05% NaN_3 at a pH of 4.0; flux: 0.4 mL/min). This system contains a pump: Waters Alliance HPLC System, and 3 detectors: a Schambeck RI detector (Bad Honnef), a light-scattering detector Wyatt MiniDawn, and a UV–VIS detector Waters Lambda-Max.

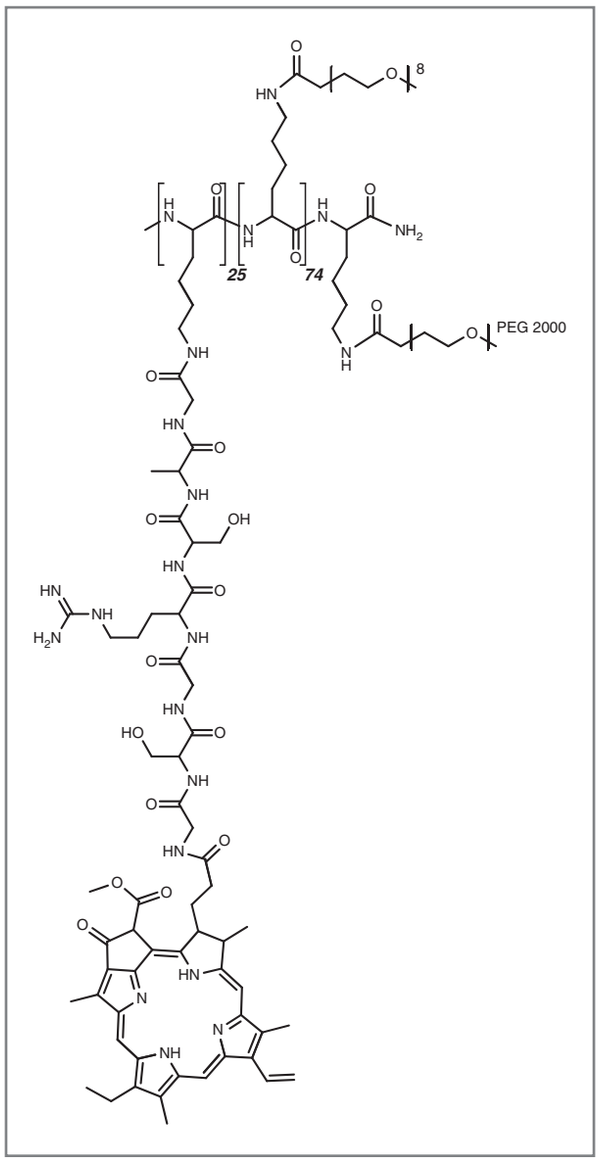

Figure 1. Schematic representation of the macromolecular prodrug uPA-PPP-4. The prodrug is synthesized with an average loading of 30% Pb*a*-peptides per polymer chain. The polymeric backbone is modified with a single high molecular weight mPEG (20 kDa) and the remaining ε-lysine residues are capped with $mPEO_8$.

Cell culture

PC-3 cells (American Type Culture Collection) from human prostate cancer origin were cultured in F-12 growth medium supplemented with 10% FBS. Luciferase-transfected PC-3M-luc-C6 cells, a kind gift of Caliper LifeSciences, were maintained in Minimum Essential Medium with Earle's Balanced Salts with 10% FBS, nonessential amino acids, L-glutamine, sodium pyruvate, and Minimum Essential Medium Vitamin Solution. Both cell lines were grown as monolayers at 37°C in a humidified incubator containing 5% CO_2. The cells were harvested using TrypLE Express, and

Published OnlineFirst December 27, 2012; DOI: 10.1158/1535-7163.MCT-12-0780

passaged every 4 to 5 days. Cell lines used in this study were not authenticated.

In vitro PDT

Phototoxicity was tested on PC-3 and luciferase-transfected PC-3M-luc-C6 cells. Aliquots of 1.2×10^4 and 1.0×10^4 cells, respectively, in 100 μL complete medium were seeded in 96-well plates and cultured for 12 hours to 70% confluence. Cells were given fresh complete medium containing uPA-PPP-4 at final concentrations of 0.5, 1.0, 2.0, 4.0, and 8.0 μmol/L Pb*a* equivalents for 6 hours. Cells were washed twice with sterile Hank's Balanced Salt Solution (HBSS) and fresh medium was added. Plates were either placed on a light table equipped with OSRAM L 18W/67 Blue light tubes (PCI Biotech) or kept in the dark. The radiation intensity was 7.5 mW/cm^2. Cells were irradiated at light doses of 2.5, 5.0, and 10 J/cm^2. Cell viability was measured using a mitochondrial MTT assay 24 hours after irradiation. First, cells were washed once with 200 μL HBSS and 50 μL MTT (1 mg/mL) in complete medium was added into each well. After 3 hours, dimethyl sulfoxide (DMSO; 200 μL) was added to dissolve formed violet formazan crystals. After brief agitation on a microplate shaker, the absorption at 525 nm was measured with a plate reader (Saphire). Positive and negative controls were treated with complete medium or 0.1% Triton in NaOH 5 mol/L, respectively. Percentage cell survival was calculated with respect to control samples, as follows: [A (test-conc.) − A (100% dead)]/[A (100% viable) − A (100% dead)] × 100. All conditions were tested in sextuplicates.

Prostate cancer model

Female swiss Nu/Nu mice (5 to 6 weeks, 17–22 g) were supplied by Charles River Laboratories. The mice were maintained with *ad libitum* access to sterile food and acidified water in a light cycled room acclimatized at 22°C ± 2°C under pathogen-free conditions. All experimental procedures on animals were carried out in compliance with the Swiss Federal Law on the Protection of the Animals, according to a protocol approved by the local veterinary authorities. To induce xenografts, 1.5×10^6 cells were injected subcutaneously into the dorsal region of mice. Tumors of approximately 200 mm^3 in size were formed within 3 weeks after inoculation.

In vivo PDT

PC-3M-luc-C6 xenograft bearing mice ($n = 7$) were injected retro-orbitally with uPA-PPP-4 (7.5 mg Pb*a* equivalents/kg) when tumors had an estimated volume of 200 mm^3 (3–4 weeks after inoculation). Tumors were irradiated with a light dose of 150 J/cm^2 at 665 ± 5 nm (Ceralas I 670, Biolitec) 16 hours after conjugate administration. The radiation intensity was 70 mW/cm^2. Animals were maintained under 1% to 2% isoflurane inhalation during irradiation. Two other groups of animals received drug alone ($n = 4$) and light alone ($n = 4$). PDT effects were followed up to 90 days by bioluminescence imaging of animals using an IVIS 200 small-animal imaging system (Caliper Life Sciences Inc.). Ten to 15 minutes before *in vivo* bioluminescence imaging, animals received an intraperitoneal injection of D-luciferin (150 mg/kg in Dulbecco's Phosphate-Buffered Saline). Mice were sacrificed when tumors reached volumes bigger than 1,000 mm^3 or at the end of the study (90 days after treatment). Data were analyzed with Living Image 3.0 software (Caliper Life Sciences Inc.).

Qualitative analysis of prodrug cleavage products

Cleavage products were qualitatively analyzed in tumor, skin, and muscle homogenates of the corresponding tissues 16 hours after systemic administration of uPA-PPP-4 (7.5 mg Pb*a* equivalents/kg). Briefly, frozen tissues were weighed and homogenized with a solution containing a protease-inhibitor cocktail (5 μL per 100 mg tissue) and acetonitrile:water (1:1; 1 mL per 100 mg tissue) by means of a tissue homogenizer (Eurostar digital IKA; Werke). The suspensions were sonicated (15 minutes at 14 kHz) and centrifuged (15 minutes at 1,450 rpm). The supernatant was collected and extraction was repeated twice as described. Collected supernatants were lyophilized and subsequently reconstituted in acetonitrile:water (1:1; 1 mL/100 mg tissue). Samples were sonicated (5 minutes, 14 kHz), filtered and subjected to analytic HPLC (LaChroma, Merck) with a fluorescence detector ($\lambda_{ex} =$ 405 nm; $\lambda_{em} = 670$ nm). Separation was conducted on a C18 column (Nucleodur gravity 3 μ CC 125/4; Macherey-Nagel) using a 0.01%TFA/water/acetonitrile gradient.

Statistical analysis

Mean ± SD values were used for expression of data. Statistical analyses of data were done using Student *t* test. Differences of $P < 0.05$ were considered statistically significant.

Results

The phototoxic effect induced by uPA-PPP-4 was investigated in the uPA-overexpressing prostate cancer cells PC-3 (19, 20) and its luciferase-expressing mutant PC-3M-luc-C6 cells. The latter was chosen for the subsequent quantitative assessment of PDT studies *in vivo*. The effect of PDT on cells treated with prodrug (0.5, 1.0, 2.0, 4.0, and 8.0 μmol/L Pb*a* equivalents), either irradiated with a light dose of 2.5, 5.0, and 10 J/cm^2 or kept in the dark is summarized in Fig. 2.

Both cell lines display a light and drug dose-dependent cell survival. uPA-PPP-4 alone presented little to no toxic effects as shown by cell survival percentages around 100% for all prodrug concentrations. Phototoxic effects were particularly evident at photosensitizer dose of 4.0 μmol/L or higher. In PC-3 cells at 8 μmol/L of Pb*a* equivalents approximately 50% of cells survived irradiation with 2.5 or 5 J/cm^2 of light, whereas at a dose of 10 J/cm^2 only 5% of cells remained viable. In PC3-3M-luc-C6 cells similar dose–response curves were observed. Cell survival after

Published OnlineFirst December 27, 2012; DOI: 10.1158/1535-7163.MCT-12-0780

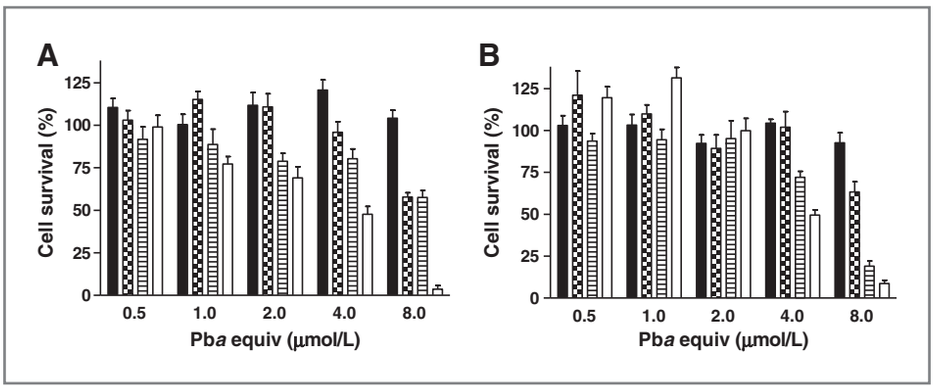

Figure 2. Light and drug dose-dependent phototoxicity induced by uPA-PPP-4 in PC-3 (A) and PC-3M-luc-C6 (B) cells. After incubation with the prodrug for 6 hours, cells were kept in the (■) dark or irradiated at (▩) 2.5 J/cm^2, (▤) 5 J/cm^2, or (□) 10 J/cm^2.

treatment with 4.0 and 8.0 μmol/L of Pb*a* equivalents at all light doses were not statistically different between PC-3 and PC3-3M-luc-C6 cells (P values > 0.05) except for the condition 8 μmol/L -5 J/cm2 (P = 2.11E-05).

We have used PC-3M-luc-C6 as basis for our experimental animal model for prostate cancer, as they allow noninvasive monitoring of tumor growth through bioluminescence in a quantitative manner (21). In this study, bioluminescence was used to assess the photodynamic efficacy of uPA-PPP-4 on tumors. Using whole body fluorescence imaging, we found that tumors became selectively fluorescent 16 hours after prodrug administration (17). Figure 3 illustrates the typical colocalization of fluorescence (rainbow-color scale) and bioluminescence (yellowhot-color scale) signals at this time point. Therefore, we selected this condition as drug-light interval in further PDT studies.

HPLC analysis of tissue extracts confirmed the presence of the expected photoactive Pb*a*-GSGR fragment inside tumors (see Fig. 4). Concentration of this compound in tumor was 27 times higher than in the skin. Some smaller fragments with longer retention times presumably due to further proteolytic processing were also found in the tumor and also to a much smaller extend in the skin. In contrast, no photoactive fragments were found in muscle.

For PDT, 7.5 mg Pb*a* equivalents/kg of prodrug was given to the mice via retro-orbital injection and 16 hours later, tumors were irradiated with 150 J/cm^2 at 665 ± 5 nm. The radiation intensity was 70 mW/cm^2. Animals receiving the drug alone or irradiated with light alone were used as controls. Figure 5A shows a sequence of images before and after PDT taken on one mouse, which ended up with complete remission. Bioluminescent images taken 15 minutes after administration of D-luciferin were used to quantify prostate cancer cells. On the average, a tumor volume of 200 mm^3 corresponds to 2.5 × 10^7 photon s^{-1}. Macroscopically, 1 day after treatment a local inflammatory response was visible. Inflammation developed into necrosis that appeared as a dark crust on the skin by day 3 and this was succeeded by healing and complete elimination of the tumor as confirmed by bioluminescence imaging. The absence of a bioluminescent signal, which persisted over 90 days, indicated complete destruction of the tumor-associated cells. Figure 5B summarizes the regions of interest analysis of sequences of images obtained for the 3 treatment regimes (PDT, drug alone, and light alone) until day 15 after treatment. Mice receiving both light and drug showed a 3 log reduction of tumor bioluminescence already the day after treatment. In this group, the mean bioluminescent signal remained below the initial value for at least 30 days (Supplementary Fig. S1). In contrast to PDT, light alone showed a slight reduction on tumor bioluminescence (P = 0.002). No reduction in bioluminescence was observed for animals

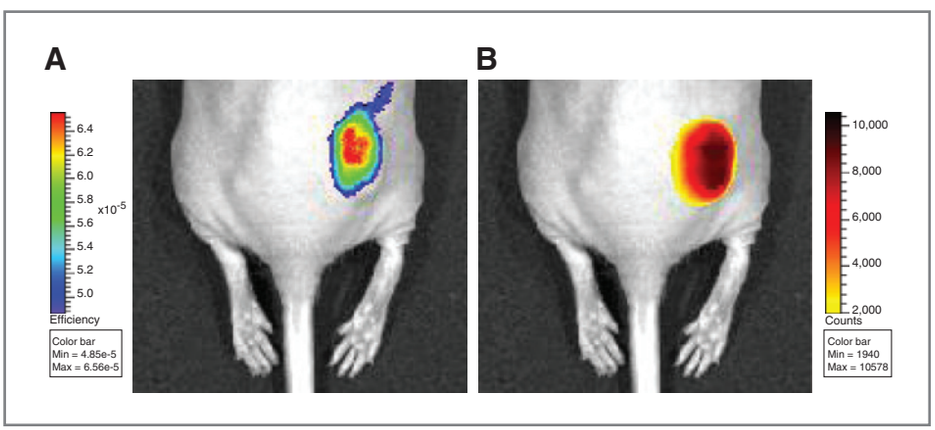

Figure 3. A, tumor fluorescence intensity 16 hours after retro-orbital administration of 2 mg/kg of uPA-PPP-4 (as Pb*a* equivalents). B, bioluminescence of luciferase-expressing PC-3M-luc-C6 tumor 15 minutes after intraperitoneal injection of D-luciferin.

Published OnlineFirst December 27, 2012; DOI: 10.1158/1535-7163.MCT-12-0780

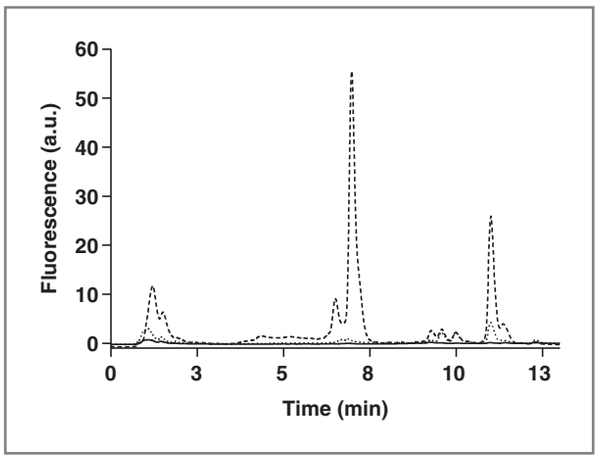

Figure 4. Analytic HPLC analysis of tumor (- -), skin (–), and muscle (—) extracts. In tumor, a major peak was found at 7.5 minutes, corresponding to the cleaved Pba-peptidyl fragment. The small peaks at 6.3 and 10 minutes are other minor cleavage Pba peptidyl fragments. The same compounds were detected in skin in trace amounts. In muscle, no cleavage products were detected at all. Chromatograms show representative traces of mouse tissues 16 hours after retro-orbital injection of uPA-PPP-4 (7.5 mg Pba equivalents/kg).

receiving prodrug alone ($P = 0.001$). In both control groups, we observed a 4-fold increase in tumor bioluminescence until day 15 after treatment, day at which the animals were euthanized. No significant difference between control groups could be established ($P = 0.6$).

The survival of mice treated with PDT, prodrug alone, and light alone is presented in Fig. 6. Animals treated with either prodrug alone or light alone had to be sacrificed before or on day 15 after treatment because of high tumor burden. The PDT survival curve was significantly different from these 2 groups ($P = 0.001$). Four animals that presented partial response to PDT were sacrificed on day 30 or 45 after treatment (57% survival). Complete remission to PDT treatment was observed in the 3 remaining mice (43% survival), which were sacrificed at the end of the study (90 days).

Discussion

Today, uPA is recognized as one of the key players in tumor progression in a wide panel of pathologies. Therefore, it has been identified as a target to specifically release cytotoxic agents. The first uPA-sensitive prodrug was reported by Chung and Kratz (22). It consisted of an albumin-bound doxorubicin containing a uPA substrate. This compound was stable in human plasma and the maximum-tolerated dose was 4.5-folds the dose of free doxorubicin as determined in a single nude mouse experiment. Subsequently, other uPA-sensitive prodrugs of TNF (23) and anthrax toxin (24) containing motifs recognized by uPA have been evaluated, providing *in vivo* evidence of potent antitumor effects. Recently, a doxorubicin analog was used for the development of an uPA-sensitive prodrug platform (25). The evaluation of one of these prodrugs in a variety of cancer cells lines showed a powerful inhibition of cell growth when activated *in vitro*.

The first polymeric photosensitizer prodrugs were developed by Choi and colleagues (26) for a more selective PDT. In this first-generation PPP, multiple copies of the photosensitizer are tethered to a protease-sensitive polymeric backbone (26, 27). A major drawback of these compounds is their limited selectivity, as all proteases recognizing a Lys–Lys motif are able to activate them. To circumvent this problem, a second-generation PPPs have been developed introducing a small peptide linker between the photosensitizer and the polymeric backbone (18). In this new design the linker-sequence is constructed according to the specific cleavage requirements of proteolytic enzymes of the target site.

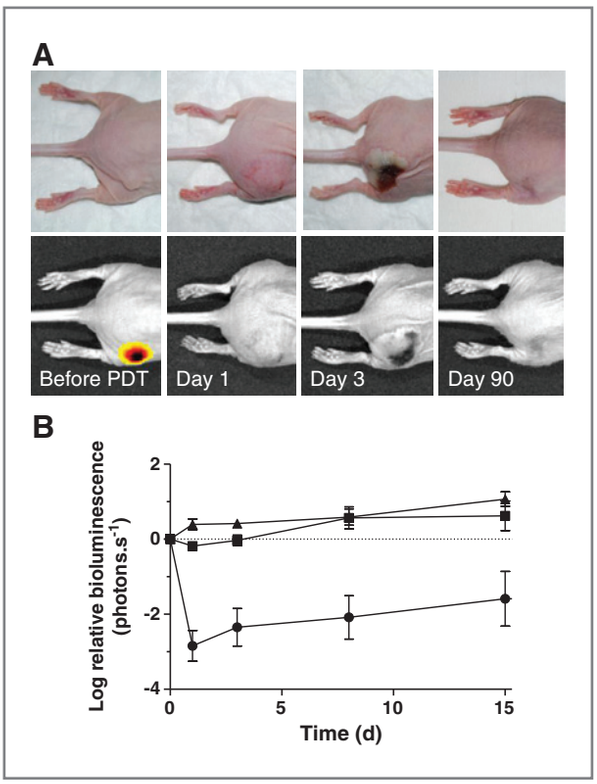

Figure 5. Treatment response was evaluated in terms of the remaining bioluminescence. A, *in vivo* imaging of a PC-3M-luc-C6 tumor-bearing mouse receiving PDT. The animal was administered with 7.5 mg Pba equivalents/kg of the prodrug and 16 hours after, the tumor was irradiated with a light dose of 150 J/cm^2 at 665 ± 5 nm. The radiation intensity was 70 mW/cm^2. Images were taken 15 minutes after peritoneal injection of D-luciferin. The intensity of the signal is correlated to cell density. The sequence on the top corresponds to the white-light images, from left to right: before, day 1, 3, and 90 after PDT. The sequence on the bottom corresponds to bioluminescent images, which confirmed total eradication of tumor cells. B, relative bioluminescence of PDT (●; $n = 7$), drug alone (▲; $n = 4$) and light alone (■; $n = 4$) groups. Tumor growth was monitored weekly by *in vivo* bioluminescence imaging. Images were taken 15 minutes after peritoneal injection of D-luciferin. Because control mice had to be sacrificed 15 days after PDT, comparison was done only for this period.

Published OnlineFirst December 27, 2012; DOI: 10.1158/1535-7163.MCT-12-0780

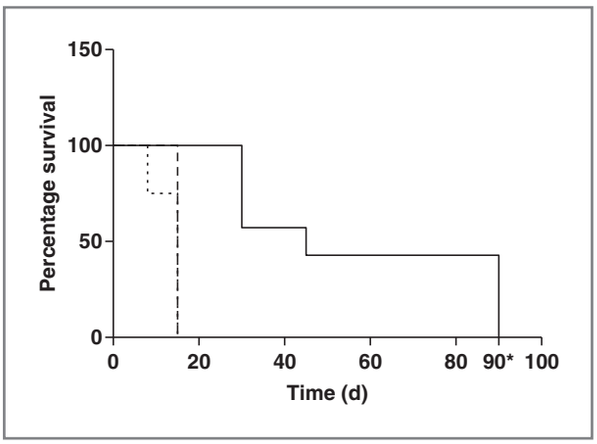

Figure 6. Survival curves in prostate cancer xenografted mice after PDT (—) as compared with control groups of light alone (– –) or drug alone (—). Animals receiving PDT were treated with 7.5 mg Pb*a* equivalents/kg of the prodrug. Sixteen hours after administration, tumors were irradiated with a light dose of 150 J/cm^2 at 665 ± 5 nm. The radiation intensity was 70 mW/cm^2. *, the study concluded after 90 days.

Because of the known overexpression of uPA in prostate cancer (16, 28), we began to explore the potential of uPA-sensitive PPPs for a selective PDT of prostate cancer. From the known uPA-sensitive substrates, we have chosen the GSGRSAG peptide sequence for our PPPs (29). These have been characterized and optimized in our laboratory in the last years (17, 30).

We have shown the selective cleavage of uPA-PPPs by uPA in the test tube and in the prostate cancer cell lines DU145 and PC-3 overexpressing this protease (30). We have further shown a selective accumulation/activation in a prostate cancer-xenograft model (17). In the present study, we combined enzymatic prodrug activation with light irradiation to obtain a phototoxic therapeutic effect. Because we have mostly used the wild-type line PC-3 for *in vitro* optimization but intended to monitor PDT effects *in vivo*, we first investigated prodrug phototoxicity with a luciferase-transfected mutant, PC-3M-luc-C6. Both cell lines were susceptible to PDT with uPA-PPP-4 and no dark toxicity was observed at the applied conditions.

Using *in vivo* fluorescence imaging, we observed a highly selective tumor fluorescence 16 hours after prodrug administration. According to a previous study comparing the tumor fluorescence after administration of the prodrug and its analogous noncleavable conjugate, this selective signal is mainly due to the site-specific proteolytic activation (17).

We further looked into the prodrug selectivity by analysis of various tissue samples for cleavage fragments. HPLC analysis of tumor tissue revealed a major peak corresponding to the Pb*a*-GRGS fragment, whereas neighboring skin contained only insignificant amounts of the cleavage product. In previous studies using orthotopic prostate cancer models, photosensitizer (benzoporphyrin derivative monoacid ring A, BPDMA) content in tissues in close proximity to the prostate including nerve, rectum, and lymph node were found to be similar to those found in skin (31). However, comparison of the photosensitizer distribution between orthotopic and subcutaneous tumors has shown significant differences (32), and therefore, the prodrug accumulation/activation in prostate surrounding tissues will need to be addressed by conducting studies in an orthotopic model.

In vivo, uPA-PPP-4 produced a strong photodynamic effect after irradiation of fluorescent PC-3M-luc-C6 tumors. Bioluminescence images show a drastic reduction of tumor cells in all animals included in the PDT group. Three animals were completely cured from prostate cancer after PDT (43% cure rate). In these animals, the total bioluminescence was reduced by 3 orders of magnitude as compared with the pretreatment images. Only few prostate cancer cells remained after treatment in 4 animals. However, tumor growth was delayed and tumors reached original volumes only 15 days after treatment or later. The phototoxic effect induced by prodrug alone and by light alone was negligible.

Successful eradication of prostate cancer bulky tumors has been also achieved with a single session of the "vascular" PDT agent, Tookad (33). Tookad is so far, one of the most studied photosensitizer in the treatment of prostate cancer and currently under clinical investigation for recurrent prostate cancer (13). In the present *in vivo* studies, our prodrug has shown results that indicate that more satisfactory outcomes of PDT can be expected in the future, thus overcoming some of Tookad's limitations. In the case of Tookad collateral damage to the urinary and rectal function has been observed in the clinical trials (12, 13).

In the present study, bioluminescence imaging helped to evaluate the tumor progression noninvasively. Furthermore, the ratio between the photon counts before PDT and 1 day after was indicative for the therapeutic outcome. This is in accordance with Fleshker and colleagues (34) who evaluated bioluminescence imaging in the treatment of breast cancer with WST11 after "vascular" PDT. We found that an average reduction of more than 3-log values was necessary to cure the animals. Thus, bioluminescence imaging can also help to improve the cure rate and adapt photodynamic treatment regimes.

To further improve the therapeutic outcome, repetitive PDT can be envisaged to address the occasional partial response. This concept of repetitive PDT has been already studied in spheroids models, *in vivo* and in the clinic mostly for the treatment of brain cancer (35–39). According to these studies, the use of multiple sessions enhanced elimination of deep tumor cells infiltrating the surrounding brain. Combination treatments might also help to improve PDT efficacy. It is now widely accepted that stress induced through photodynamic insult in certain cases initiates signaling pathways, leading to VEGF increase in prostate cancer cells (40), which in turn contributes to tumor survival and regrowth. In this context,

Published OnlineFirst December 27, 2012; DOI: 10.1158/1535-7163.MCT-12-0780

PDT in combination with antiangiogenic agents for prostate cancer might result in an increased anticancer response.

Conclusions

We developed a uPA-sensitive prodrug that is not toxic to prostate cancer cells but efficiently inactivates cells *in vitro* after enzymatic activation and exposure to light. Activation of the prodrug occurs selectively in the tumors and is correlated with uPA overexpression. *In vivo* PDT can completely eliminate prostate cancer xenografts as shown by bioluminescence imaging. More research in orthotropic prostate cancer models is envisioned to confirm the potential advantages of our strategy over other current PDT approaches.

Disclosure of Potential Conflicts of Interest

No potential conflicts of interest were disclosed.

Authors' Contributions

Conception and design: D. Gabriel, H. van den Bergh, N. Lange
Development of methodology: M.-F. Zuluaga, D. Gabriel, H. van den Bergh, N. Lange
Acquisition of data (provided animals, acquired and managed patients, provided facilities, etc.): M.-F. Zuluaga, N. Sekkat, N. Lange
Analysis and interpretation of data (e.g., statistical analysis, biostatistics, computational analysis): M.-F. Zuluaga, N. Lange
Writing, review, and/or revision of the manuscript: M.-F. Zuluaga, D. Gabriel, H. van den Bergh, N. Lange
Administrative, technical, or material support (i.e., reporting or organizing data, constructing databases): H. van den Bergh
Study supervision: N. Lange

Grant Support

This work was supported by the Swiss National Science Foundations grants: 205320-122144, 205321_126834, K-32K1-116460, IZLSZ2_123011, and Diabetes.

The costs of publication of this article were defrayed in part by the payment of page charges. This article must therefore be hereby marked *advertisement* in accordance with 18 U.S.C. Section 1734 solely to indicate this fact.

Received July 30, 2012; revised October 26, 2012; accepted December 3, 2012; published OnlineFirst December 27, 2012.

References

1. Jemal A, Bray F, Center MM, Ferlay J, Ward E, Forman D. Global cancer statistics. CA Cancer J Clin 2011;61:69–90.
2. Ahmed HU, Pendse D, Illing R, Allen C, van der Meulen JH, Emberton M. Will focal therapy become a standard of care for men with localized prostate cancer? Nat Clin Pract Oncol 2007;4:632–42.
3. Ahmed HU, Moore C, Emberton M. Minimally-invasive technologies in uro-oncology: the role of cryotherapy, hifu and photodynamic therapy in whole gland and focal therapy of localised prostate cancer. Surg Oncol 2009;18:219–32.
4. Pinthus JH, Bogaards A, Weersink R, Wilson BC, Trachtenberg J. Photodynamic therapy for urological malignancies: past to current approaches. J Urol 2006;175:1201–7.
5. Moore CM, Hoh IM, Bown SG, Emberton M. Does photodynamic therapy have the necessary attributes to become a future treatment for organ-confined prostate cancer? Br J Urol Int 2005;96:754–8.
6. Windahl T, Andersson SO, Lofgren L. Photodynamic therapy of localised prostatic cancer. Lancet 1990;336:1139.
7. Moore CM, Nathan TR, Lees WR, Mosse CA, Freeman A, Emberton M, et al. Photodynamic therapy using meso tetra hydroxy phenyl chlorin (mthpc) in early prostate cancer. Lasers Surg Med 2006;38:356–63.
8. Zaak D, Sroka R, Höppner M, Khoder W, Reich O, Tritschler S, et al. Photodynamic therapy by means of 5-ala induced ppix in human prostate cancer—preliminary results. Med Laser Appl 2003;18:91–95.
9. Lepor H. Vascular targeted photodynamic therapy for localized prostate cancer. Rev Urol 2008;10:254–61.
10. Verigos K, Stripp DCH, Mick R, Zhu TC, Whittington R, Smith D, et al. Updated results of a phase I trial of motexafin lutetium-mediated interstitial photodynamic therapy in patients with locally recurrent prostate cancer. J Environ Pathol Toxicol Oncol 2006;25:373–88.
11. Patel H, Mick R, Finlay J, Zhu TC, Rickter E, Cengel KA, et al. Motexafin lutetium-photodynamic therapy of prostate cancer: short- and long-term effects on prostate-specific antigen. Clin Cancer Res 2008;14:4869–76.
12. Trachtenberg J, Bogaards A, Weersink RA, Haider MA, Evans A, McCluskey SA, et al. Vascular targeted photodynamic therapy with palladium-bacteriopheophorbide photosensitizer for recurrent prostate cancer following definitive radiation therapy: assessment of safety and treatment response. J Urol 2007;178:1974–9.
13. Trachtenberg J, Weersink RA, Davidson SR, Haider MA, Bogaards A, Gertner MR, et al. Vascular-targeted photodynamic therapy (padoporfin, wst09) for recurrent prostate cancer after failure of external beam radiotherapy: a study of escalating light doses. Br J Urol Int 2008;102:556–62.
14. Arumainayagam N, Moore CM, Ahmed HU, Emberton M. Photodynamic therapy for focal ablation of the prostate. World J Urol 2010;28:571–6.
15. Maeda H, Wu J, Sawa T, Matsumura Y, Hori K. Tumor vascular permeability and the epr effect in macromolecular therapeutics: a review. J Control Release 2000;65:271–84.
16. Cozzi PJ, Wang J, Delprado W, Madigan MC, Fairy S, Russell PJ, et al. Evaluation of urokinase plasminogen activator and its receptor in different grades of human prostate cancer. Hum Pathol 2006;37:1442–51.
17. Zuluaga MF, Gabriel D, Lange N. Enhanced prostate cancer targeting by modified protease sensitive photosensitizer prodrugs. Mol Pharm 2012;9:1570–9.
18. Gabriel D, Campo MA, Gurny R, Lange N. Tailoring protease-sensitive photodynamic agents to specific disease-associated enzymes. Bioconjug Chem 2007;18:1070–7.
19. Sehgal I, Forbes K, Webb MA. Reduced secretion of mmps, plasminogen activators and timps from prostate cancer cells derived by repeated metastasis. Anticancer Res 2003;23:39–42.
20. Forbes K, Gillette K, Kelley LA, Sehgal I. Increased levels of urokinase plasminogen activator receptor in prostate cancer cells derived from repeated metastasis. World J Urol 2004;22:67–71.
21. Jenkins DE, Yu SF, Hornig YS, Purchio T, Contag PR. *In vivo* monitoring of tumor relapse and metastasis using bioluminescent pc-3m-luc-c6 cells in murine models of human prostate cancer. Clin Exp Metastasis 2003;20:745–56.
22. Chung DE, Kratz F. Development of a novel albumin-binding prodrug that is cleaved by urokinase-type-plasminogen activator (upa). Bioorg Med Chem Lett 2006;16:5157–63.
23. Gerspach J, Nemeth J, Munkel S, Wajant H, Pfizenmaier K. Target-selective activation of a tnf prodrug by urokinase-type plasminogen activator (upa) mediated proteolytic processing at the cell surface. Cancer Immunol Immunother 2006;55:1590–600.
24. Rono B, Romer J, Liu SH, Bugge TH, Leppla SH, Kristiansen PEG. Antitumor efficacy of a urokinase activation-dependent anthrax toxin. Mol Cancer Ther 2006;5:89–96.
25. Barthel BL, Rudnicki DL, Kirby TP, Colvin SM, Burkhart DJ, Koch TH. Synthesis and biological characterization of protease-activated prodrugs of doxazolidine. J Med Chem 2012;55:6595–607.
26. Choi Y, Weissleder R, Tung CH. Selective antitumor effect of novel protease-mediated photodynamic agent. Cancer Res 2006;66:7225–9.

Published OnlineFirst December 27, 2012; DOI: 10.1158/1535-7163.MCT-12-0780

27. Campo MA, Gabriel D, Kucera P, Gurny R, Lange N. Polymeric photosensitizer prodrugs for photodynamic therapy. Photochem Photobiol 2007;83:958–65.
28. Shariat SF, Roehrborn CG, McConnell JD, Park S, Alam N, Wheeler TM, et al. Association of the circulating levels of the urokinase system of plasminogen activation with the presence of prostate cancer and invasion, progression, and metastasis. J Clin Oncol 2007;25:349–55.
29. Ke SH, Coombs GS, Tachias K, Navre M, Corey DR, Madison EL. Distinguishing the specificities of closely related proteases. Role of p3 in substrate and inhibitor discrimination between tissue-type plasminogen activator and urokinase. J Biol Chem 1997;272:16603–9.
30. Gabriel D, Zuluaga MF, Martinez MN, Campo MA, Lange N. Urokinase-plasminogen-activator sensitive polymeric photosensitizer prodrugs: design, synthesis and *in vitro* evaluation. J Drug Deliv Sci Tec 2009; 19:15–24.
31. Momma T, Hamblin MR, Wu HC, Hasan T. Photodynamic therapy of orthotopic prostate cancer with benzoporphyrin derivative: local control and distant metastasis. Cancer Res 1998;58:5425–31.
32. Chen B, Pogue BW, Zhou X, O'Hara JA, Solban N, Demidenko E, et al. Effect of tumor host microenvironment on photodynamic therapy in a rat prostate tumor model. Clin Cancer Res 2005;11:720–7.
33. Koudinova NV, Pinthus JH, Brandis A, Brenner O, Bendel P, Ramon J, et al. Photodynamic therapy with pd-bacteriopheophorbide (tookad): successful *in vivo* treatment of human prostatic small cell carcinoma xenografts. Int J Cancer 2003;104:782–9.
34. Fleshker S, Preise D, Kalchenko V, Scherz A, Salomon Y. Prompt assessment of wst11-vtp outcome using luciferase transfected tumors enables second treatment and increase in overall therapeutic rate. Photochem Photobiol 2008;84:1231–7.
35. Madsen SJ, Sun CH, Tromberg BJ, Hirschberg H. Repetitive 5-aminolevulinic acid-mediated photodynamic therapy on human glioma spheroids. J Neurooncol 2003;62:243–50.
36. Bogaards A, Varma A, Zhang K, Zach D, Bisland SK, Moriyama EH, et al. Fluorescence image-guided brain tumour resection with adjuvant metronomic photodynamic therapy: pre-clinical model and technology development. Photochem Photobiol Sci 2005;4:438–42.
37. Hirschberg H, Sorensen DR, Angell-Petersen E, Peng Q, Tromberg B, Sun CH, et al. Repetitive photodynamic therapy of malignant brain tumors. J Environ Pathol Toxicol Oncol 2006;25:261–79.
38. Zilidis G, Aziz F, Telara S, Eljamel MS. Fluorescence image-guided surgery and repetitive photodynamic therapy in brain metastatic malignant melanoma. Photodiagnosis Photodyn Ther 2008;5:264–6.
39. Mathews MS, Angell-Petersen E, Sanchez R, Sun CH, Vo V, Hirschberg H, et al. The effects of ultra low fluence rate single and repetitive photodynamic therapy on glioma spheroids. Lasers Surg Med 2009; 41:578–84.
40. Solban N, Selbo PK, Sinha AK, Chang SK, Hasan T. Mechanistic investigation and implications of photodynamic therapy induction of vascular endothelial growth factor in prostate cancer. Cancer Res 2006;66:5633–40.

AACR American Association for Cancer Research

Molecular Cancer Therapeutics

Selective Photodetection and Photodynamic Therapy for Prostate Cancer through Targeting of Proteolytic Activity

Maria-Fernanda Zuluaga, Nawal Sekkat, Doris Gabriel, et al.

Mol Cancer Ther 2013;12:306-313. Published OnlineFirst December 27, 2012.